ARCHIVIO ISTITUZIONALE
DELLA RICERCA

Alma Mater Studiorum Università di Bologna
Archivio istituzionale della ricerca

Efficient and thermally stable BHJ solar cells based on a soluble hydroxy-functionalized regioregular polydodecylthiophene

This is the final peer-reviewed author's accepted manuscript (postprint) of the following publication:

Published Version:
Lanzi M., Pierini F. (2021). Efficient and thermally stable BHJ solar cells based on a soluble hydroxy-functionalized regioregular polydodecylthiophene. REACTIVE & FUNCTIONAL POLYMERS, 158, 1-12 [10.1016/j.reactfunctpolym.2020.104803].

Availability:
This version is available at: https://hdl.handle.net/11585/790273 since: 2021-01-21

Published:

DOI: http://doi.org/10.1016/j.reactfunctpolym.2020.104803

Terms of use:

Some rights reserved. The terms and conditions for the reuse of this version of the manuscript are specified in the publishing policy. For all terms of use and more information see the publisher's website.

This item was downloaded from IRIS Università di Bologna (https://cris.unibo.it/).
When citing, please refer to the published version.

(Article begins on next page)

08 November 2026

This is the final peer-reviewed accepted manuscript of:
M. Lanzi, F. Pierini, *Efficient and thermally stable BHJ solar cells based on a soluble hydroxy-functionalized regioregular polydodecylthiophene*,React. Funct. Polym., 158 (2021) 104803 p. 1-12

The final published version is available online at:

https://doi.org/10.1016/j.reactfunctpolym.2020.104803

Rights / License:

The terms and conditions for the reuse of this version of the manuscript are specified in the publishing policy. For all terms of use and more information see the publisher's website.

This item was downloaded from IRIS Università di Bologna (https://cris.unibo.it/)

When citing, please refer to the published version.

Efficient and thermally stable BHJ solar cells based on a soluble hydroxy-functionalized regioregular polydodecylthiophene

Massimiliano Lanzi[*,†] *and Filippo Pierini*[§]

[†]Department of Industrial Chemistry "Toso Montanari", Alma Mater Studiorum-University of Bologna, 40136 Bologna, Italy

[§]Department of Biosystems and Soft Matter, Institute of Fundamental Technological Research, Polish Academy of Sciences, Warsaw 02-106, Poland

Highlights

- A soluble hydroxy-substituted polythiophene was synthesized.
- The functionalization enhances thermal and morphological properties.
- Optimized BHJ solar cell nanomorphology improves efficiency.
- Long-term stability of devices is due to interchain hydrogen bond.

Keywords:

Bulk heterojunction solar cell

Regioregular polythiophene derivatives

Post-polymerization functionalization

Over-time stability

Graphical abstract

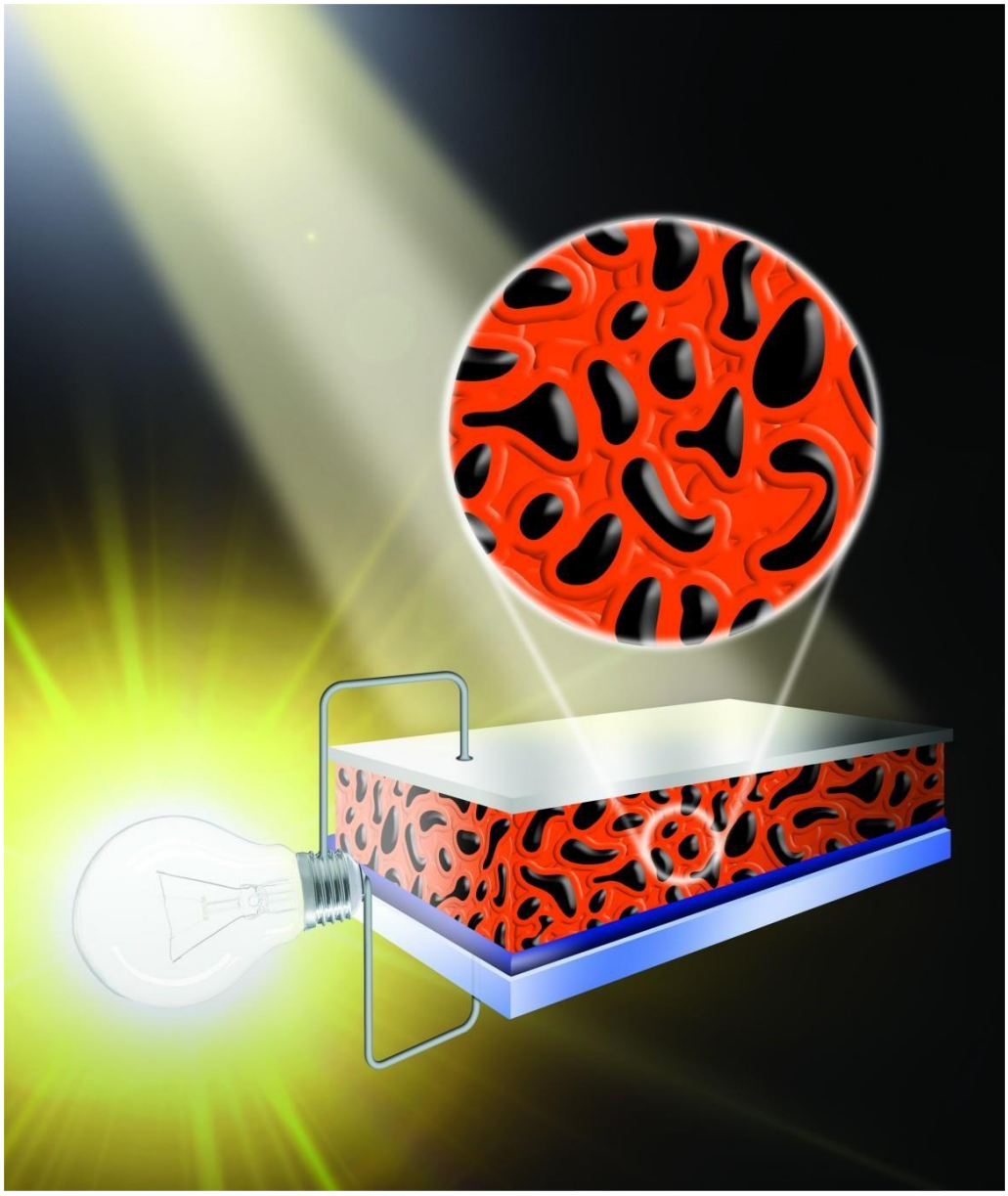

Schematic view of the prepared BHJ solar cells

Abstract

A new regioregular polythiophene derivative, called poly[3-(12-hydroxydodecyl)thiophene] (PT12OH), was synthesized by post-functionalizing its ω-brominated precursor poly[3-(12-bromododecyl)thiophene] (PT12Br) prepared using the Grignard metathesis route. Thanks to the

optimal balance between hydrophilic and hydrophobic groups within its structure, PT12OH was highly soluble and easily filmable from common organic solvents allowing for its complete characterization. It also showed enhanced thermal properties, crystallinity, and self-assembling capabilities by the formation of strong inter- and intrachain hydrogen bonds. Bulk heterojunction photovoltaic cells with PT12OH and $PC_{61}BM$ showed a PCE of 4.83% and a remarkable over-time stability, offering good photoconversion efficiency even after 120 h of accelerated aging. Indeed, the PCE decrease was 34% for the hydroxylated polymer and 65% for its brominated precursor. It should also be pointed out that the enhanced thermal stability of PT12OH was achieved without resorting to any complex post-annealing photochemical, thermal, or chemical treatment and was thus directly ascribable to the polymer chemical structure. The simple and effective synthetic procedure, photovoltaic efficiency, and enhanced stability revealed the potential of PT12OH for large-scale organic solar cell applications.

1. Introduction

Conjugated polymer/fullerene solar cells have been studied in depth and their progress has been rapid over the past decade. The main strengths of these devices are their light weight, flexibility, low cost, and the ability to be filmed easily on large surfaces. The structure most commonly adopted is the bulk heterojunction (BHJ), which consists of a physical mixture of a conjugated polymer as the electron- donor (ED) and a fullerene derivative as the electron- acceptor (EA). Electron- transfer from the ED component by the fast separation of strongly linked photo-generated excitons to the EA component, and the subsequent fast transport of free charges to the respective electrode, are the key features of this kind of architecture [1]. In an ideal device, the optimized ED/EA physical blend should provide a large interface contact area in order to generate a high number of free-charge carriers and a bicontinuous blend morphology to efficiently transport them to each electrode at the same time [2]. However, an optimized 3D-nanomorphology of the photoactive blend is not easy to obtain, since the two components usually exhibit phase-separated structures,

resulting in poor devices performance. Indeed, the ED-EA final blend morphology is driven by the kinetic freezing of a non-equilibrium state during the film deposition on the cell substrate. The poor miscibility of the two components often leads to the formation of fullerene domains within the polymeric matrix, whose dimensions are larger than the exciton diffusion length on the polymer (usually 10 nm). Thermal annealing is used to control phase-separation since both polymer and EA component tend to crystallize during the heating process, forming a nanoscale interpenetratednetwork which is able to effectively increase the performance of the final device [3]. The achieved nanomorphology, however, is not thermally stable and tends spontaneously to induce macrophase separation when exposed to heat during photoefficiency measurements (exposition to solar simulator light) or the final use (exposition to direct sunlight). This is not only determined by the scarce miscibility of ED/EA components but also by the relatively low phase- transitions temperatures usually shown by the conjugated polymers used (e.g. poly(3-hexylthiophene), P3HT). In order to reduce EA aggregation, some authors synthesized chemically- crosslinkable fullerene derivatives containing glycidyl functionality [4,5] or photocrosslinkable group-side chain functionalized polythiophenes [6] with the aim of freezing polymer film morphology immediately after the thermal annealing procedure.

Long flexible alkyl side chains have been recently used for single-component organic solar cells, in which the alkylic chain is exploited to link the electron donor (located in the conjugated backbone) and the electron acceptor in pendant side groups [7], Moreover, longer alkyl (dodecyl) linkers between ED and EA units also improved the crystallinity of the synthesized double-cable polymers compared to shorter alkyl linkers [8]. According to Yang et al. [9], the length of alkyl side chains hasa significant impact on the conformational order and crystallization of poly(3-alkylthiophene)s (P3AT)s. For example, poly(3-dodecylthiophene) (P3DDT) shows a higher solubility in organic solvents than its shorter side-chain counterparts, and its main chain can assume ordered conformations despite the side- chain lengths. Moreover, for regioregular head-to-tail (HT) samples,

the interactions between the interdigitated alkylic chains can lead to a planarization process in which the angle of the adjacent thiophenic rings decreases gradually, creating rod-like extended chains [10]. Indeed, the DSC analysis of regioregular P3DDT evidenced the presence of a sharp main-chain crystallization peak (at 114°C) and a broad one peaked at 59°C, due to the side- chain crystallization during cooling [11]. Interchain associations, providing a high degree of supramolecularorganization, have also been found in P3DDT diluted solutions [12]. Some authors have reported onthe existence of a liquid crystalline state after the melting of side chains forP3DDT [13, 14] and recently, Liu et al. [15] evidenced that the structure evolution of P3DDT DSC peaks during the heating scan can be ascribed to subsequent melting and recrystallization processes.Lastly, P3DDT also exhibited good electrical conductivity and marked solvatochromic and thermocromic effects [16,17].

Poly(3-alkylthiophene)s (P3AT)s ω-functionalized with a bromine atom in alkylic side chains are versatile polymers, soluble in a wide range of organic solvents. They can be further functionalized using simple and quantitative nucleophilic substitution reactions. Moreover, long linear side chains, introduced as internal plasticizers to improve the solubility of polythiophenes, thus making solution-processing easier, do not deprive the polyconjugated backbone of the possibility to yield strong π-π associations (π-stacking) and weaker Van der Waals interactions along different directions [18]. Furthermore, the possibility for P3ATs to self-assemble through the interactions andcrystallization of (long) linear side chains is particularly enhanced for samples with a high configurational regularity. In view of this, we have synthesized the regioregular poly[3-(12- bromododecyl)thiophene] (PT12Br), which was converted to PT12OH by a simple alkaline methanolysis reaction, and their solutions were mixed with [6,6]-phenyl-C61-butyric acid methyl ester (PCBM) to obtain photoactive layers. After the annealing procedure, the -OH functionality should enhance the conformational stability of polymeric chains through interchain hydrogen bonds, thus increasing the over-time performance of the photovoltaic devices prepared. Moreover,

dodecylic side chains can also increase polymer solubility, making the deposition of polymer/PCBM photoactive layers easier.

Scheme 1a shows the synthetic pathway adopted to obtain PT12OH, while Scheme 1b shows the structure of the prepared polymeric BHJ solar cells. Synthesized polymers were completely characterized using chemical and spectroscopic techniques, and the power conversion efficiency of some polymer/PCBM BHJ solar cells was evaluated using an AM 1.5 one-sun solar simulator. Lastly, the overtime stability was carefully evaluated, showing that PT12OH exhibited an excellent stability under thermal stress, which may be ascribed to its enhanced resistance to microstructure variations. Indeed, after accelerated aging tests, the decrease in the power conversion efficiency of PT12OH was twice as low as that of its precursor PT12Br.

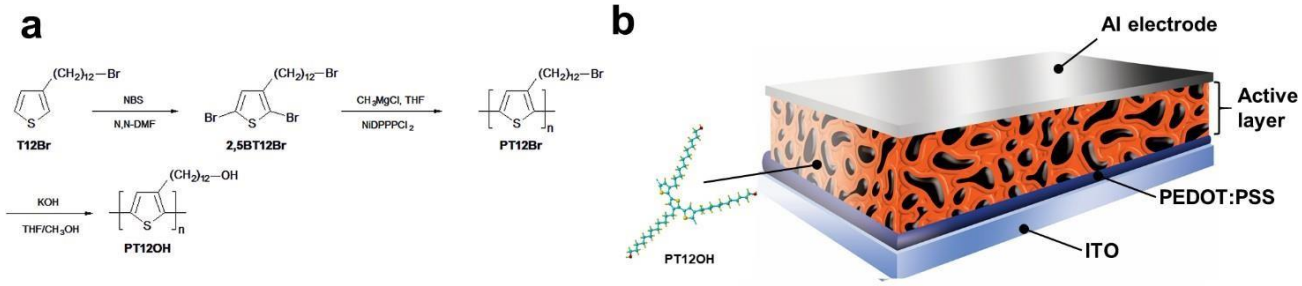

Scheme 1. Synthesis of the polymer PT12OH (a) and schematic view of polymeric BHJ solar cells (b).

2. Experimental section

2.1. Materials

All commercially available reagents were used as received without purification unless otherwise stated. All solvents used (HPLC grade) were dried and purified by conventional laboratory procedures, stored over molecular sieves and handled in a moisture-free atmosphere.

2.2. Measurements

^{1}H- and ^{13}C-NMR were recorded on a Varian Mercury Plus (400 MHz) spectrometer using TMS as a reference. IR spectra were taken on Ge disks using a Perkin Elmer Spectrum One or a Bruker Alpha Platinum spectrophotometer. UV-Vis absorption spectra were recorded on a Perkin Elmer Lambda 19 spectrophotometer using 10^{-5} M polymer solutions in spectroquality solvents in Suprasilquartz cuvettes (1 cm × 1 cm) or films on quartz slides. Emission spectra were recorded using an Edinburgh FLSP 920 spectrofluorimeter and samples were prepared as described for absorbance spectra. Molecular weights were determined by gel permeation chromatography (GPC) using $CHCl_3$ solutions on a HPLC Lab Flow 2000 apparatus equipped with a Rheodyne 7725i injector, aPhenomenex Mixed bed column 5μ MXL and a Linear Instruments UVIS-200 detector operating at 254 nm. The calibration curve was recorded using monodisperse polystyrene standards. A DSC TA Instruments Q2000 was used for the thermal analysis by varying the temperature from -50°C to 250°Cat a rate of 10°C min^{-1} in a nitrogen atmosphere. A TGA TA Instruments Q600, operating in air flux,was used to determine the decomposition temperatures of the samples by heating from30°C upto 900°C at a scan rate of 10°C min^{-1}. Cyclic voltammograms were recorded using an Autolab PGSTAT204 (Metrohm) potentiostat/galvanostat at a potential scan rate of 100 mV/s on polymer films deposited on glassy carbon disk (GC) electrodes from $CHCl_3$ solutions. The working electrode(GC disk), the counter electrode (Pt wire), and the reference electrode (aqueous saturated calomel electrode) were immersed in an acetonitrile solution with tetrabutylammonium hexafluorophosphate(TBAPF6) 0.1 M as the supporting electrolyte using a single compartment three-electrode cell. The morphology and energy dispersive X-ray (EDX) spectroscopic analyses in active layers were performed using a scanning electron microscope (SEM; CrossBeam 350, Carl Zeiss, Germany) equipped with an EDX system. The samples were coated with a 5 nm-thick gold layer using a sputter coater before observation. Atomic force microscopy (AFM) measurements were made on a Ntegra (NT-MDT) system equipped with a rectangular silicon cantilever (HA_NC,

NT-MDT, nominal spring constant of 12 N/m, and tip curvature radius smaller than 10 nm) in tapping modes in order to analyse the morphology of active materials. The root mean squared (RMS) surface roughness of the samples was measured analysing ten AFM topographies (3 μm x 3 μm) for each material using Nova software. X-ray diffraction data of polymer films were recordedat room temperature by using a CuKα (λ = 1.5406 Å) radiation source (Philips PW 1050) and a Bragg-Brentano diffractometer (Philips PW 1710) equipped with a graphite monochromator in the diffracted beam. The 2θ range between 2.0 and 90.0° was scanned by 881 steps of 0.1° with a counting time of 15 s for each step.

BHJ solar cells were prepared according to the following procedure: the ITO glass substrate (1 cm × 1 cm, surface resistance 21 Ω/sq) was etched on one side by using a 10% wt aqueous solution of HCl and heated at 60°C for 15 min in order to obtain an area of 0.75 × 1 cm covered by indium tin oxide. The glass was then cleansed in an ultrasonic bath (Elmasonic S30H) using acetone and treated at 60°C for 20 min with a solution of aqueous NH_3 (0.8 M) and H_2O_2 (0.5 M), rinsed with distilled water, 2-propanol, and dried with a nitrogen flow. The final resistance of the ITO glass was 12 Ω/sq. Poly(3,4-ethylenedioxythiophene):polystyrene sulfonic acid (PEDOT:PSS, 2.8 wt% dispersion in water, viscosity 20 cps) was diluted 1:1 v/v with 2-propanol, sonicated, and filtered on a Gooch G2, and the resulting solution (viscosity 12 cps) was deposited on the previously treated ITO glass by the doctor blading technique using a Sheen Instrument Model S265674, leaving only asmall (0.25 × 1 cm) area uncovered on the opposite side of the previously etched area. The PEDOT:PSS film was heated in a Büchi GKR-50 glass oven at 130°C for 2 h under vacuum (10^{-3} mmHg). A solution made by mixing 5 mg of polymer and 6.25 mg of PCBM in 2 ml of chlorobenzenewas sonicated for 15 min, filtered on a PTFE septum (0.40 μm pore size) and deposited by doctor blading on the slide in order to cover the PEDOT:PSS layer. The sample was then annealed in the glass oven under vacuum (10^{-3} mmHg) at 150°C for 10 min. Finally, a 50 nm thick Al electrode wasdeposited over the polymeric layer through a shadow mask using an

Edwards 6306A coating system operating at 10^{-6} mmHg. The active area of the cell was 0.25 × 0.25 cm^2. The current-voltage characteristics were measured in air using a Keithley 2401 source meter under the illumination of an Abet Technologies LS150 Xenon Arc Lamp Source AM 1.5 Solar Simulator (100 mW/cm^2) calibrated with an ILT 1400-BL photometer. The structure of the final devices was: ITO (80 nm)/PEDOT:PSS (100 nm)/active layer (150 nm)/Al (50 nm). The spectral response of the solar cells was measured using a 7-SC Spec III Modularized Solar Cell SpectralTest System (SevenStar Optics, Beijing, PRC). Layer thicknesses were measured using a Film Thickness Probe FTPAdvances FTPadv-2 (Sentech GmbH, Germany) equipped with the FTPExpertsoftware.

2.3. Monomer and polymer synthesis

2,5-Dibromo-3-(12-bromododecyl)thiophene (2,5BT12Br)

8.00 g (24.1 mmol) of 3-(12-bromododecyl)thiophene (T12Br), prepared according to Refs. 19,20, were dissolved in 30 ml of anhydrous N,N-dimethylformamide (DMF), and 4.28 g (24.1 mmol) of N-bromosuccinimide (NBS) in 30 ml of DMF were added dropwise. After reacting for 6 h at 20°C in the dark under inert atmosphere, another portion of NBS was added dropwise (6.43 g, 36.1 mmol in 35 ml of DMF). The mixture was stirred for 24 h at room temperature, diluted with 800 ml of distilled water and extracted several times with n-heptane (5×300 ml). The collected organic phases were dried and concentrated, yielding 9.05 g (18.5 mmol) of 2,5BT12Br. After the purification of the crude product by column chromatography (silica gel, n-heptane) 7.97 g (16.3 mmol) of colourless oil were recovered (68% yield).

^{1}H-NMR ($CDCl_3$, ppm): δ 6.76 (1H, s); 3.44 (2H, t); 2.51 (2H, t); 1.87 (2H, m); 1.61-1.55 (6H, m); 1.43-1.25 (12H, bm).

^{13}C-NMR ($CDCl_3$, ppm): δ 143.43; 131.64; 112.18; 107.91; 35.22; 33.85; 32.78; 29.64; 29.53; 29.41; 29.29; 28.77; 28.34; 28.15; 28.01; 27.93.

FT-IR (KBr, cm^{-1}): 3084, 2935, 2852, 1544, 1463, 1429; 1416, 1255, 1003, 827, 644, 562, 474.

Mass spectrum: MS(ES+) 489 (22 M^+); 270 (55, $C_6H_6Br_2S$); 256 (90, $C_5H_4Br_2S$).

Poly[3-(12-bromododecyl)thiophene] (PT12Br)

Methylmagnesium chloride (1.02 ml, 3.0M) in THF was added to a solution of 1.50 g (3.06 mmol) of 2,5BT12Br in 25 ml of anhydrous THF. The mixture was refluxed for 2 h under argon and 8.29 mg (0.015 mmol) of [1,3-(bis-diphenylphosphino)propane] Ni(II) chloride ($NiDPPPCl_2$) were addedand the reaction mixture was refluxed for one more hour. The polymer was recovered from the orange solution by adding 400 ml of methanol and subsequent filtering on a PTFE membrane (0.40 μm pore size). The recovered polymer was dissolved in 15 ml of $CHCl_3$, precipitated again with 100 ml of methanol, filtered, and dried under vacuum, yielding 0.67 g (2.03 mmol, 66% yield) of a dark orange powder.

^{1}H-NMR ($CDCl_3$, ppm): δ 6.98 (1H, s); 3.42 (2H, t); 2.80, 2.55 (2H, 2bm); 1.75 (2H, m); 1.56 (6H, bm); 1.34 (12H, m).

^{13}C-NMR ($CDCl_3$, ppm): δ 141.88; 134.65; 133.88; 128.56; 35.17; 33.91; 32.61; 29.56; 29.17; 29.13; 29.06; 28.63; 28.22; 28.13; 27.95; 27.89.

FT-IR (Ge, cm^{-1}): 3055, 2928, 2855, 1560, 1513, 1460, 1437, 1258, 1233, 1041, 832, 728, 645, 561, 518.

Elemental analysis: Calcd. for $(C_{16}H_{25}BrS)_n$: C 58.35; H 7.65; Br 24.26; S 9.74; Found: C 58.11; H 7.87; Br 24.32; S 9.70.

Poly[3-(12-hydroxydodecyl)thiophene] (PT12OH)

0.66 g (2.00 mmol) of PT12Br were dissolved in 35 ml of THF and 65 ml of a 10% (m/v) solution of KOH in methanol were then added dropwise over 1 h at room temperature under stirring. The reaction mixture was refluxed for 3 h, cooled down to room temperature and added with 250 ml of methanol. After neutralization, the precipitated polymer was recovered by centrifugation (4000 rpm for 20 min) and the obtained dark purple solid was washed with fresh methanol, yielding 0.50 g (1.88 mmol) of PT12OH (94% yield).

^{1}H-NMR ($CDCl_3$/CD_3OD, 0.16 CD_3OD m.f., ppm): δ 7.02 (1H, s); 3.53 (2H, t); 2.82, 2.58 (2H, 2bm); 1.74 (2H, m); 1.55 (6H, bm); 1.35 (12H, m).

^{13}C-NMR ($CDCl_3$/CD_3OD, 0.16 CD_3OD m.f., ppm): δ 142.21; 135.32; 134.22; 129.97; 63.22, 33.76; 33.25; 29.90; 29.78; 29.53; 29.28; 28.88; 28.34; 28.15; 27.88; 27.12.

FT-IR (Ge, cm^{-1}): 3375, 3054, 2926, 2851, 1508, 1459, 1382, 1258, 1155, 1119, 1056, 882, 818, 716.

Elemental analysis: Calcd. for $(C_{16}H_{26}OS)_n$: C 72.12; H 9.84; O 6.00; S 12.04; Found: C 71.83; H 10.12; O 5.81; S 12.24.

3. Results and discussion

The synthesis of PT12Br is shown in Scheme 1a. The intermediate 3-(12-bromododecyl)thiophene (T12Br) was selectively dibrominated in the 2,5 positions of the aromatic ring with N-bromosuccinimide (NBS) in N,N-dimethylformamide (DMF) according to an optimized two-steps procedure. The dibrominated product 2,5-dibromo-3-(12-bromododecyl)thiophene (2,5BT12Br)

was reacted with one equivalent of methylmagnesium chloride in anhydrous THF under reflux. After 2 h, the catalyst [1,3-bis(diphenylphosphino)propane] Ni(II) chloride ($NiDPPPCl_2$) was added to activate the coupling step according to the Grignard metathesis (GRIM) procedure developed by McCullough for the synthesis of regioregular PATs [21,22]. After refluxing for one more hour, the regioregular polymer PT12Br was recovered by filtration and subsequent reprecipitation with a good yield (66%, Table 1).

PT12Br was highly soluble in common organic solvents (up to 15 mg/ml in $CHCl_3$ and in THF) and was subjected to a post-polymerization functionalization reaction using KOH in a THF/CH_3OH mixture, yielding the hydroxy-functionalized polymer PT12OH (94% yield, Table 1). PT12OH was soluble in $CHCl_3$ (up to 5 mg/ml), fairly soluble in THF (about 0.5 mg/ml) and completely soluble in $CHCl_3$/MeOH 0.16 methanol molar fraction (up to 13 mg/ml). This solvent mixture already proved to have strong solvating power towards hydroxy-functionalized polyalkylthiophenes [23].On the one hand, the co-presence of low-polar (methylenes) and high polar (-OH) groups on the same (side) chain reduces the solubility of PT12OH in $CHCl_3$ and in THF but, on the other, permits the formation of intra- and intrachain hydrogen bonds which can stabilize the conformational order of the polymeric backbone, thus increasing the main chain conjugation length and rendering the final properties steadier.

Table 1

Polymer characteristics

Polymer	Yield (%)[a]	HT (%)[b]	M_n (KDa)[c]	M_w/M_n	DPn
PT12Br	66	98	36.2	1.23	110
PT12OH	94	98	29.3	1.31	110

[a] In fractionated polymer.

[b] Regioregularity expressed as head-to-tail dyad percentage, determined by means of ^{1}H-NMR spectrometry.

[c] Determined by GPC relatively to polystyrene standards

The synthesized polymers were first characterized by ^{1}H- and ^{13}C-NMR (Fig. 1).

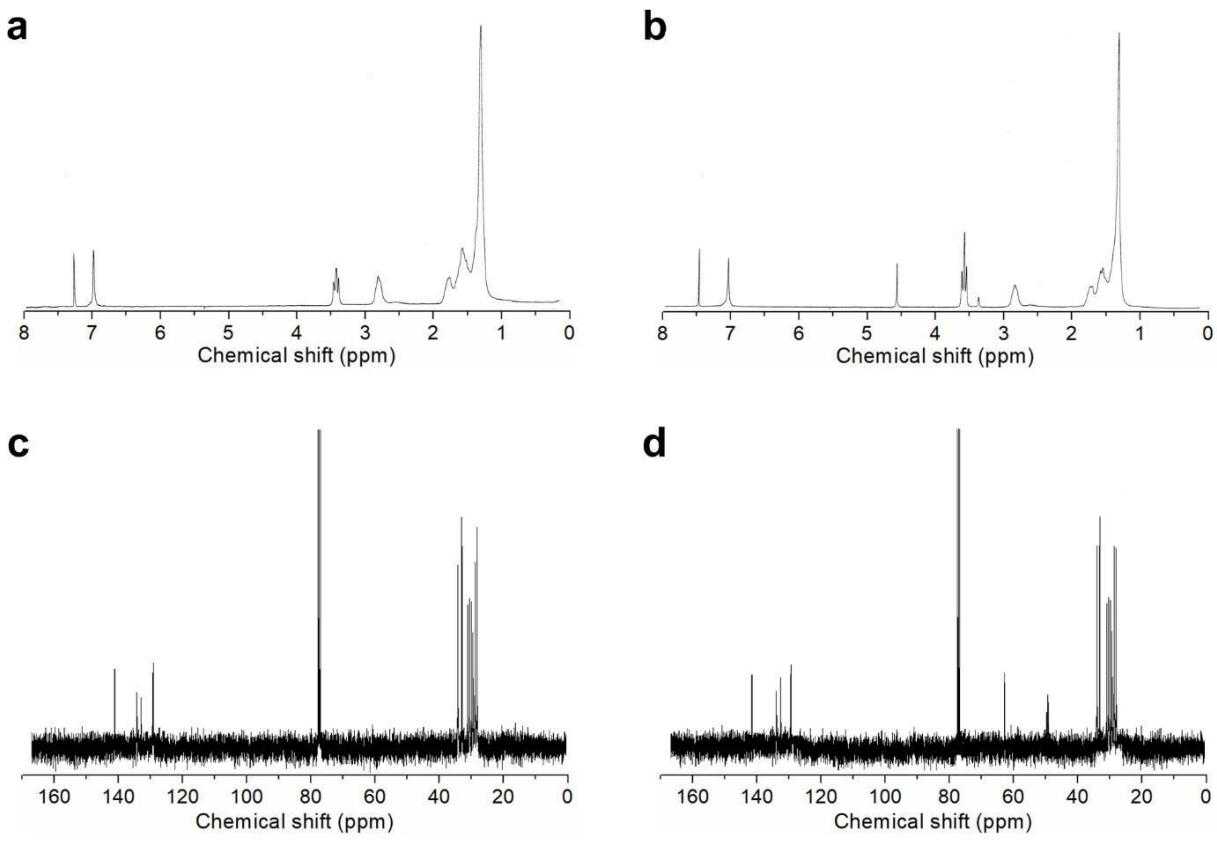

Fig. 1. ^{1}H-NMR spectra of PT12Br (a), PT12OH (b) and ^{13}C-NMR spectra of. PT12Br (c) and PT12OH (d).

The spectra show a singlet in the aromatic region at 6.98 ppm for PT12Br (Fig. 1a) and at 7.02 ppm for PT12OH (Fig. 1b), which can be ascribed to the H-4 thiophenic proton. The absence of signals attributable to H-2 and H-5 aromatic protons suggests that polymers are obtained at relatively high molecular weight (i.e. no signals ascribable to chain ends can be found). Furthermore, the fact that the signal in the aromatic zone is a singlet, suggests that polymers have a high regioregularity degree. The regioregularity can also be easily determined by considering the resonance of methylenic protons α to the thiophene ring. In fact, this resonance is split into two signals (at 2.80 and 2.55 ppm for PT12Br and at 2.82 and 2.58 ppm for PT12OH) which can be ascribed to the dyads originating from different monomer couplings: the peak at lower fields may be attributed to head-to-tail (HT) junctions, while the other to head-to-head and tail-to-tail (HH, TT) linkages.

Therefore, the regioregularity of polymers is given by the ratio of their integrated intensities: 98%

HT for both polymers (Table 1), in good agreement with the values usually reported for GRIM polymerization of 3-substituted alkylthiophene monomers. Finally, the complete conversion of –Br functionality is evidenced by the missing of the signal at 3.42 ppm (-C*H*$_2$Br) and the appearance of the peak at 3.53 ppm (-C*H*$_2$OH) passing from the PT12Br to the PT12OH ^{1}H-NMR spectrum.

According to ^{1}H-NMR analysis, ^{13}C-NMR spectra of polymers (Fig. 1, c and d) show only four signals in the aromatic region (142-128 ppm range) which can be ascribed to thiophenic carbons of the prevailing HT-HT configurational triad. In addition, the signal at 35.17 ppm (-*C*H$_2$Br) is substituted by the resonance at 63.22 ppm (-*C*H$_2$OH), further confirming the expected substitution of the side-chain functional group. In order to obtain more detailed spectra, NMR of PT12OH were recorded in the $CDCl_3$/CD_3OD 0.16 CD_3OD molar fraction (m.f.) mixture (about 10:1 v/v), a system which proved to have a strong solvating power towards hydroxy-functionalized polyalkylthiophenes [24]. Methanol-*d*$_4$ signals can be found at 4.55 and 3.38 ppm (Figure 1b) and 49.25 ppm (Figure 1d).

Polymers were also characterized by FT-IR spectroscopy using thin films on a germanium disk; the recorded spectra are reported in Fig. 1SI. PT12Br spectrum shows the absence of the band at 1003 cm^{-1} (thiophene α-Br stretching), which is clearly evident in 2,5BT12Br monomer, while in the PT12OH spectrum, the aliphatic C-Br stretching bands at 645 and 561 cm^{-1} are substituted by the evident absorption at 3375 cm^{-1} (O-H stretching), thus confirming that the expected chemical structures are obtained.

The comparison between the position of the peaks ascribable to CH_2 asymmetric and symmetric stretching modes - characteristic of the alkyl side chains of the two polymers - shows that they are located at 2928 and 2855 cm^{-1} for PT12Br and 2926 and 2851 cm^{-1} for PT12OH, respectively. The peak position of these bands is sensitive to the packing level of alkylic side chains and shifts to lower wavenumbers when the chains become more ordered [25]. Moreover, the intensity ratios of the IR bands assigned to the symmetric and antisymmetric stretching of the thiophene ring (at about

1460 and 1510 cm^{-1}) are 2.75 for PT12Br and 2.12 for PT12OH. The lower value obtained for the -OH functionalized polymer may be related to its more extended conjugation along the polymeric backbone [26]. Finally, the absorptions relative to the C-H out-of-plane bending of tri-substituted thiophenes show a marked shift from 832 (PT12Br) to 818 cm^{-1} (PT12OH), indicating a higher order and crystallinity for the latter polymer [27]. These findings clearly suggest that the hydroxy-functionalized polymer is able to attain more ordered conformations in the film state compared to its brominated precursor.

Gel permeation chromatography (GPC) analysis reveals the same polymerization degree (DP_napprox. 110 repeating units) for the two polymers, in agreement with the fact that PT12OH was obtained by post-functionalizing PT12Br with a reaction that does not involve the polymericbackbone. Very low polydispersity indices also bear out the effectiveness of the purification and fractionation procedures adopted for crude polymers (Table 1). GPC traces are shown in Fig. 2. Thepresence of a small shoulder in the PT12OH peak at higher molecular weights, which can not be detected for the PT12Br sample, may be ascribed to a small amount of aggregates due to the lower solubility of the hydroxylated polymer in the elution solvent ($CHCl_3$).

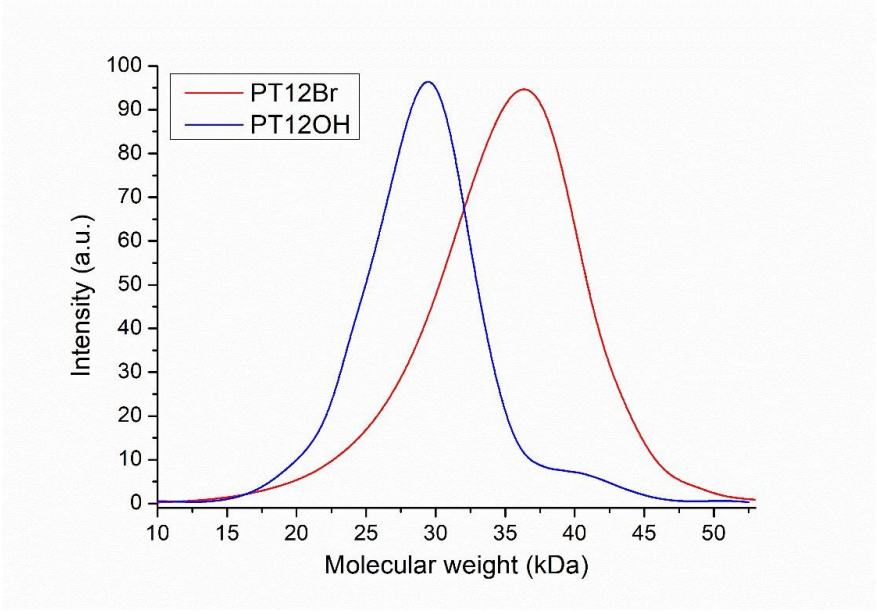

Fig. 2. GPC eluograms of PT12Br and PT12OH

3.1. Optical properties

The study of the chromic phenomena of P3ATs in a solution is an important tool for analysing the relationship between backbone conformation and electronic structure. In fact, any conformational change causes a modification in the conjugation length and hence to a shift in the UV-Vis spectrum. For example, a bathochromic shift (or red-shift) of the maximum absorption wavelength (λ_{max}) and a marked structuration of the spectral profile can be found when the conjugated backbone attains an increased planarity and the resulting chromophore is more conjugated than the pristine one.

Planar assemblies are usually induced by adding poor solvents to polymer solutions in goodsolvents, lowering the temperature or passing from the solution to the solid (film) state. Planarization drives polymer chains towards more rigid, stacked, and linear conformations, thus determining the chromic behaviour of the polymer. UV-Vis spectra of PT12Br and PT12OH in chloroform at increasing methanol concentration are shown in Fig. 3a and Fig. 3b, respectively.

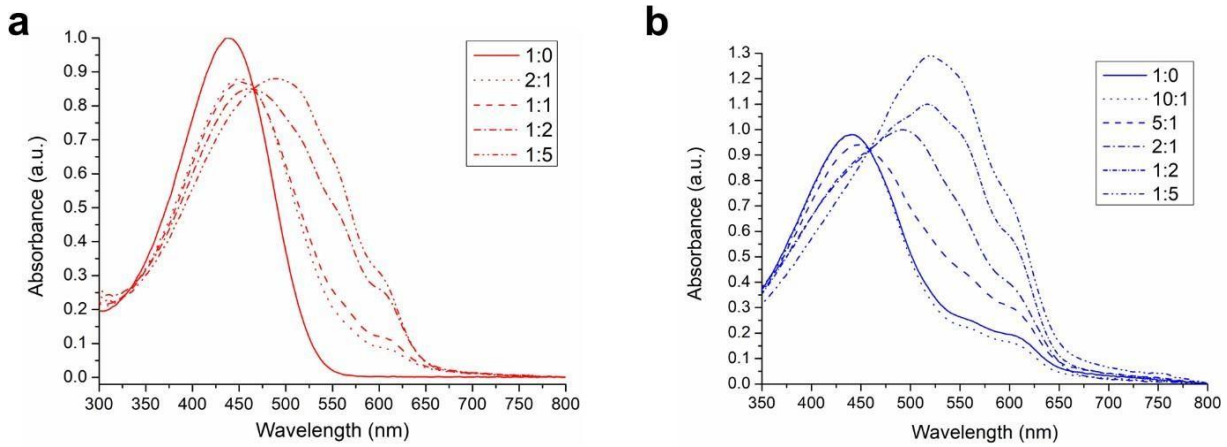

Fig. 3. UV-Vis spectra of PT12Br (a) and PT12OH (b) in $CHCl_3/CH_3OH$ at increasing non-solvent (methanol) volume ratio. Polymer concentration was kept constant at 5×10^{-5} M.

The presence of an isosbestic point indicates the coexistence in the solution of two distinct chromophores having different conjugation lengths: a shorter one, at high energies and high $CHCl_3$ content, which is a characteristic of highly solvated chains, and a longer one, in excess of poor

solvent (CH_3OH), which may be ascribed to less solvated and more conjugated conformers. PT12Br undergoes an evident solvatochromic effect with a $\Delta\lambda_{max}$ of 50 nm (from 437 to 487 nm, passing from pure $CHCl_3$ to the mixture with the highest methanol content) while for PT12OH, thisbathochromic shift is even more marked ($\Delta\lambda_{max}$ = 80 nm, from 440 to 520 nm). Moreover, the $E_{0\text{-}0}$ pure electronic transition can be found at about 594 nm for the brominated polymer and at 604 nm for the hydroxylated one. For PT12OH a very small ipsochromic shift (from 440 to 439 nm) was also observed passing from pure $CHCl_3$ to the $CHCl_3/CH_3OH$ 10:1 v/v mixture. The apparent hyperchromic effect observed for PT12OH solutions with high methanol content may also be ascribed to the polymer extended π-conjugation when examined in this solvent/non-solvent system [28].

Solvatochromism is an ideal system for studying the self-assembling capabilities of macromolecules, which are left free to undergo intra-chain interactions in the examined diluted solutions, thus promoting the generation of microaggregated species and, at the same time, providing important information on the possible behaviour of the polymer in the solid state [29]. Therefore, we can argue that PT12OH is an especially suitable polymer for optoelectronic applications, being able to achieve highly planar conformations with a high electronic delocalization. Enhanced planarizing interactions, due to inter- and intra-chain hydrogen bonds, leading to an extended conjugation length for the PT12OH sample, are also suggested by the comparison between the UV-Vis spectra of the synthesized polymers in the solid (film) state shown in Fig. 4.

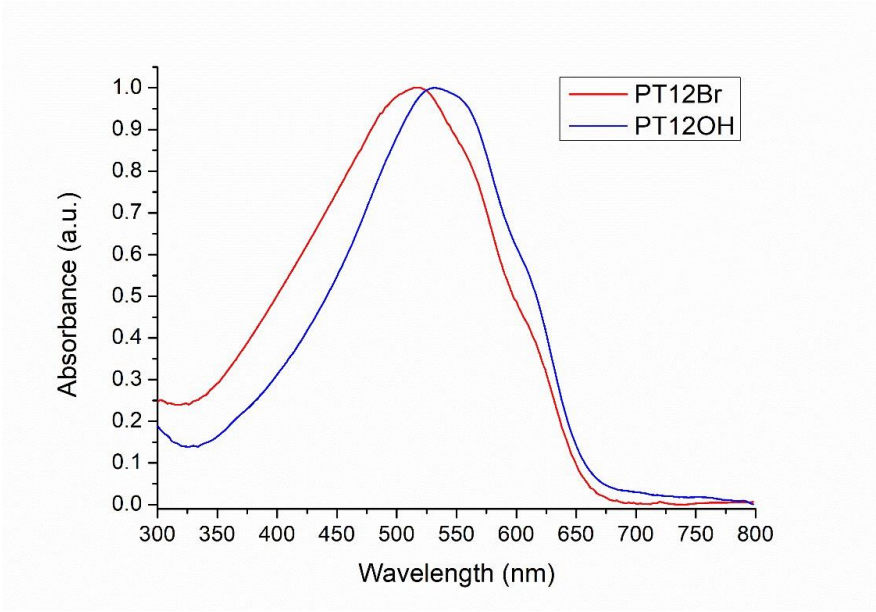

Fig. 4. UV-Vis spectra of PT12Br and PT12OH in film cast from $CHCl_3$ solution.

Indeed, in the solid state, the absorption of the conjugated backbone was found at 514 nm for PT12Br and 531 nm for PT12OH, corresponding to a mean conjugation length of 13 and 16 conjugated thiophenes, respectively. These values were obtained using the semi-empirical relation found by Jiang [30], which relates the length of conjugated π-electron structure n_L with the wavenumber of the absorption peak in the UV-Vis spectrum:

$$\nu = A - B(1/2)^{n_L^2}$$

where A and B are constants determined for the different conjugated polymers.

Furthermore, the presence of significant shoulder at 607 nm (PT12Br) and 614 nm (PT12OH), which can be ascribed to the 0-0 pure electronic transition ($E_{0\text{-}0}$), suggests the existence of crystalline domains in both polymers, since this absorption is only evident in conformational ordered polythiophenic chains which are able to form interchain π-π stacking in the solid state [31]. Moreover, the conjugation length of the polymeric backbone, which is strongly related to the presence of ordered conformers, is inversely proportional to the W parameter, which represents the free exciton bandwidth of the polymeric aggregates. W can be measured by the ratio of the

absorbance ascribable to 0-0 and 0-1 vibronic transitions in the UV-Vis spectra of polythiophenes [32] using the following expression:

$$\frac{A_{0-0}}{A_{0-1}} = \left| \frac{1 - 0.24 W / E_p}{1 + 0.073 W / E_p} \right|^2$$

where E_p is the main intramolecular vibration coupled to the electronic transition [33]. The deconvolution of the spectral profiles shown in Fig. 4 made it possible to carefully evaluate the position of the first vibronic quantum (0-1) (Fig. 2SI), found at 553 and 559 nm for PT12Br and PT10OH, respectively. The calculated W values were 0.171 for the brominated polymer and 0.145 for the hydroxylated sample, once again suggesting a higher conformational order and crystallinity for PT12OH.

The emission spectra of the synthesized polymers in $CHCl_3$ solution and in the solid (film) state are shown in Fig.s 5a and Fig. 5b, respectively. All compounds are characterized by large Stokes shifts from absorption to emission (Table 2).

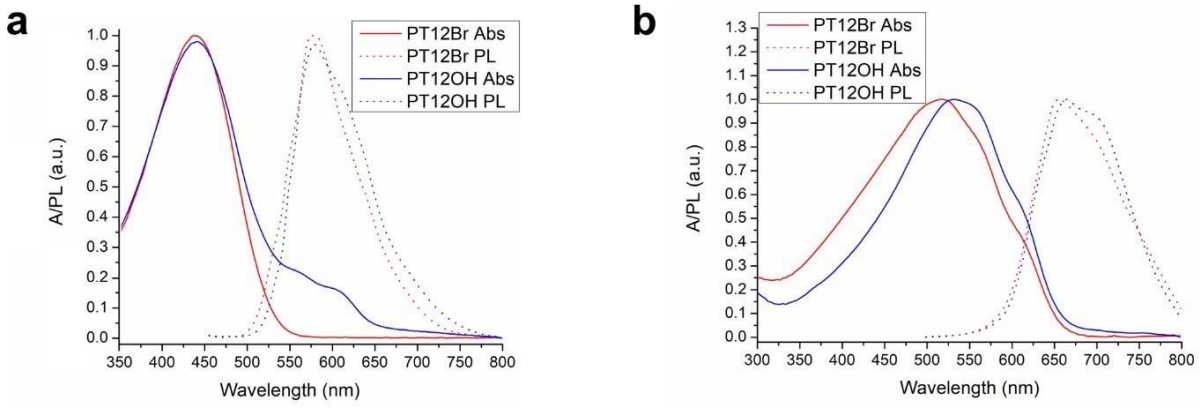

Fig. 5. Normalized absorption and PL spectra of PT12Br and PT12OH in $CHCl_3$ (a) and film (b).

Stokes shift values of the two examined samples are very similar both in the solution and in the film, but the difference in the maximum wavelength of emissions between the two polymers is lower than that recorded for absorption: in the solution, $\Delta\lambda_{max}$ is 2 nm for absorption and 0 nm for emission, whereas it is 17 nm and 6 nm for polymer films, respectively. This fact can be explained interms of nuclear geometry changes in the chromophores, passing from an aromatic structure (in the fundamental state, with an average interannular bond order, IB, near 1) to a quinoid one (in the excited state, with an IB near 2). This structural change has important consequences, leading to a more planar conformation in the excited state, while the energy dissipated during the existence ofthe latter can be measured by the Stokes shift. PT12Br exhibits larger Stokes shifts than PT12OH, since planarizing interchain interactions for the former are more evident in the excited state than in the ground state, while the latter shows a higher degree of coplanarity in polymeric chains alreadyin the fundamental state [34].

Table 2. Absorption and emission maximum wavelength of polymers in $CHCl_3$ solution and film

Sample	$\lambda_{max,abs}$ (nm)	$\lambda_{max,PL}$ (nm)	shift (nm)
PT12Br (solution)	437	572	135
PT12Br (film)	514	670	156
PT12OH (solution)	439	572	133
PT12OH(film)	531	676	145

3.2. Electrochemical properties

The electrochemical properties of polymers were examined using the cyclic voltammetry (CV) technique. Voltammograms were recorded by spin-coating polymer solutions on a glassy carbon

disk electrode (Fig. 3SI). Considering that the SCE reference electrode has a potential of 4.40 eV relative to vacuum [35], the energy of the HOMO and LUMO levels was then estimated according to the relations:

$$E_{HOMO} = -e(E_{ox}^{onset} + 4.40)\ eV \quad E_{LUMO}$$

$$= -e(E_{red}^{onset} + 4.40)\ eV$$

As reported in Table 3, PT12Br and PT12OH show especially low HOMO level energies compared to the standard reference P3HT (-4.8 eV [36]), this makes it easier to obtain a high open-circuit voltage, being the V_{oc} of a BHJ solar cell directly proportional to the absolute value of I_p(HOMO) [37]. Moreover, the electrochemical bandgaps are also very low, with positive potential implications on the conversion efficiency of the photovoltaic cells [38].

Table 3. Polymer electrochemical characteristics

Sample	E_{ox}^{onset} (V)	E_{red}^{onset} (V)	E_g^{ec} (eV)	HOMO (eV)	LUMO (eV)	λ_{onset} (nm)	E_g^{opt} (eV)
PT12Br	0.90	-0.84	1.74	-5.30	-3.56	642	1.93
PT12OH	0.85	-0.80	1.65	-5.25	-3.60	651	1.90

It is worth mentioning that the difference between the optical and electrochemical bandgap (usually amounting to a few tenths of eV) can be ascribed to the exciton binding energy, which is built into the optical bandgap [39]. Indeed, only the electrochemical bandgap value can be adopted as a

representative bandgap energy at infinite chain length [40].

3.3. Thermal properties

The thermal stability of polymers was determined by the thermogravimetric analysis (TGA). The weight loss in an air environment with a heating scan of 10°C/min is shown in Fig. 4SI. PT12Br is thermally stable up to 245°C and PT12OH up to 275°C with the subsequent loss of the functional group inserted at the end of the dodecyl chain. The second and third weight losses can be ascribed to the random side chain scission and backbone combustion, respectively.

The DSC analysis was conducted under nitrogen atmosphere with a heating rate of 10°C/min (Fig. 5SI). The DSC thermograms of the two polymers are very similar, showing two endothermic peaks during the heating scan and two exothermic peaks during the cooling scan. The peaks at lower temperatures can be ascribed to side- chain melting and crystallization, while those found at higher temperatures are ascribable to the same phase transitions, but involving the polymeric main chain. No evident glass transition was found for both samples.

Table 4. Thermal characteristics[a] of polymer samples

Polymer	T_{m1} (°C)	T_{m2} (°C)	T_{c1} (°C)	T_{c2} (°C)	ΔH_{m1} (J/g)	ΔH_{m2} (J/g)	ΔH_{c1} (J/g)	ΔH_{c2} (J/g)
PT12Br	44	136	38	75	5.21	6.28	4.83	6.81
PT12OH	65	171	60	104	5.93	6.87	5.11	7.27

a) $T_{m1}/\Delta H_{m1}$ = side-chain melting temperature/enthalpy; $T_{m2}/\Delta H_{m2}$ = main-chain melting temperature/enthalpy; $T_{c1}/\Delta H_{c1}$ = side-chain crystallization temperature/enthalpy ; $T_{c2}/\Delta H_{c2}$ = main-chain crystallization temperature/enthalpy.

PT12OH shows transition temperatures and ΔH values higher than PT12Br both for melting and crystallization phase transitions (Table 4), and this is probably due to its higher crystallinity degree.

3.4. Diffraction properties

In order to study the molecular arrangement of polymer films, X-ray diffraction (XRD) patterns were recorded and are shown in Fig. 6. The films examined showed three characteristic peaks at the small angles assigned to (100), (200), and (300) reflections, respectively (Table 5). The first order reflection (100) may be ascribed to the distance between the polythiophenic chains on the same plane, while (200) and (300) peaks are induced by multiple X-ray reflections by the film. The *d*- spacing corresponding to the distance between the thiophene molecules belonging to the sameplane, observed in PT12Br and PT12OH samples (26.31 and 26.22 Å, respectively), is shorter with respectto the double of the calculated side chain length (30.21 and 30.64 Å), as determined by the density functional theory (DFT) for the B3LYP/6-31G(d) level. This indicates that side chains are partially interdigitated, providing a three-dimensional chain ordering which can result in enhanced charge-transport properties [41]. Moreover, the less evident peaks at wide angles (2θ = 22.91 and 23.15 degrees for PT12Br and PT12OH, respectively), partially embedded within the broad amorphous halo and ascribable to the presence of π-π stacking of the thiophene rings in the main chains, once again confirms the semicrystalline nature of the two polymers suggested by DSC analysis.

The comparison between the mean size of polymer crystallites (*L*) in the two samples, evaluated using Scherrer's equation [42] (Table 5), indicates that the hydroxylated polymer is characterizedby larger crystalline domains than those observed for its brominated precursor. The crystallization process of PT12OH is probably made easier by a more planar conformation in the solid state driven by inter- and intrachain hydrogen bond interactions which can reduce the side chain flexibility, thus

decreasing the rotational freedom of the polymeric backbone. These observations are in line with the reported thermal characteristics of the hydroxylated polymer as compared to those of its brominated precursor. Indeed, the latter can not exploit any stabilizing interaction between side chains, being functionalized with a cumbersome halogen group.

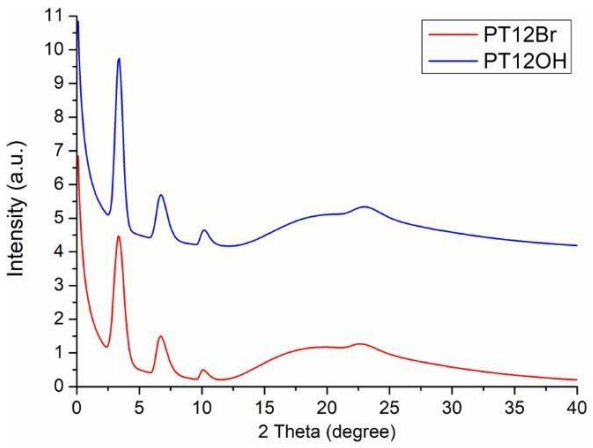

Fig. 6. X-Ray diffractograms of PT12Br and PT12OH in film

Table 5. Structural parameters of polymers

Sample	Low-angle diffractions (2θ) (degrees)	High-angle diffractions (2θ) (degrees)	On-plane Th chain distances (Å)	Plane stacking distances (Å)	Crystallite mean sizes (*L*) (nm)
PT12Br	3.35; 6.72; 10.12	22.91	26.31	3.85	10.58
PT12OH	3.37; 6.74; 10.18	23.15	26.22	3.81	11.46

3.5. Photovoltaic measurements

Polymers were used to fabricate some photovoltaic cells using a physical blend of PT12Br or PT12OH (electron donor, ED) and $PC_{61}BM$ (electron acceptor, EA). The photoluminescence (PL) spectra of the polymer/PCBM blends were recorded to evaluate the most appropriate ED/EA ratio forpreparing efficient BHJ cells. For example, the P3HT/PCBM mass ratio should be higher than 1:0.75in order to achieve an appreciable power conversion efficiency (PCE>2.5%) [43], even though thereis no clear indication in literature for the upper limit for PCBM content. In view ofthis, we recorded the PL spectra of both PT12Br-based (Fig. 7a) and PT12OH-based (Fig. 7b) blends, cast from chlorobenzene, having different polymer/PCBM weight ratios: 1:0.75, 1:1, 1:1.25,and 1:1.50 w/w. The emission spectra of these blends were recorded after the annealing procedure (150°C for 10 minunder vacuum) in order to simulate the conditions adopted for the preparation of final BHJ solar cells.

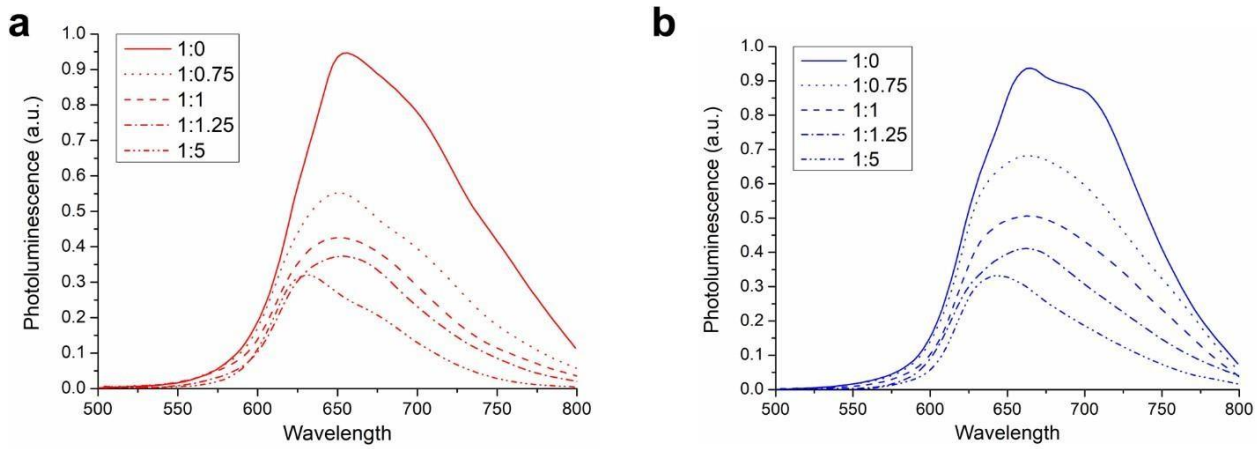

Fig. 7. Photoluminescence spectra of PT12Br (a) and PT12OH (b) blend films at different polymer:PCBM weight ratio.

The progressive reduction in the PL intensity may be ascribed to the efficient photoinduced charge-separation between ED (polymer) and EA (PCBM) molecules [44]. At higher EA content (1:1.5 w/w) a marked red-shift in the maximum absorption wavelength of the emission spectrum can be

found for both polymers, thus suggesting that the higher content of PCBM can disrupt the ordered intermolecular packing structure of the conjugated polymer. Therefore, we chose to prepare the photoactive blend using a 1:1.25 polymer/PCBM weight ratio.

A series of BHJ solar cells with the structure ITO (80 nm)/PEDOT:PSS (100 nm)/polythiophene (PT12Br or PT12OH):PCBM (150 nm)/Al (50 nm) was prepared following the conditions described in the Experimental section, in order to investigate the photoconversion efficiency of the synthesized polymers as photoactive layers. Current density (J) –voltage (V) curves corresponding to the devices which gave the best performances (PCE_{best}) recorded under AM 1.5 one-sun illumination (100 mW/cm^2) are shown in Fig. 8, and the main photovoltaic parameters (short-circuitcurrent density J_{sc}, open-circuit voltage V_{oc}, fill factor FF and power conversion efficiency PCE) based on the measurements of ten devices are collected in Table 6.

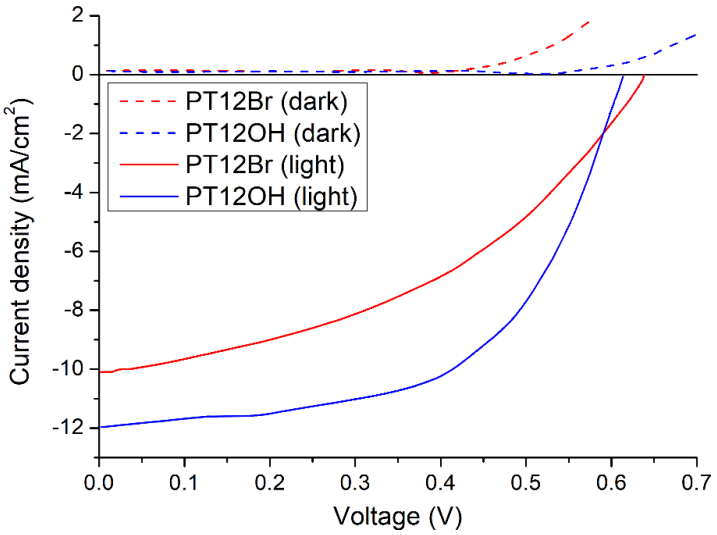

Fig. 8. Current density/voltage for the best-performing cells in the dark and under AM 1.5 one-sun illumination.

Table 6. Photovoltaic characteristics of the cells (average performances taken from ten devices) under AM 1.5 one-sun illumination.

Sample	J_{sc} (mA cm^{-2})	V_{oc} (V)	FF	PCE (%)	PCE_{best} (%)
PT12Br	9.89±0.4	0.64±0.01	0.59±0.02	3.77±0.16	3.92
PT12OH	11.5±0.5	0.61±0.01	0.64±0.03	4.51±0.18	4.83

Photoactive polymer/PCBM 1:1.25 (w/w) blends were subjected to heat treatment (150°C for 10 min under vacuum) in order to optimize their morphology. We chose a short heating time since longer periods may result in PCE degradation caused by micron-scale PCBM crystallization which can lead to a progressive segregation of the EA component from the ED polymeric matrix [45]. On the one hand, PT12Br shows the higher V_{oc} between the two examined polymers, which is probablydue to its lower HOMO level [46], but on the other, it has a wider bandgap when compared to PT12OH (1.74 eV vs. 1.65 eV, respectively). Moreover, the brominated polymer absorbs very weakly in the long wavelength range (λ>500 nm), while the absence of hydrogen bond interactions renders a less solid state order than the hydroxylated counterpart. Consequently, the device usingthe PT12Br blend shows lower J_{sc} and FF values, resulting in a less effective photoconversion of theincident light. Thisis also consistent with the reduced charge recombination determined by a better nanophase separationof PT12OH/PCBM blend [8]. Furthermore, the dark current under forward bias (Fig. 8) is higher for PT12OH than for PT12Br, suggesting a decreased series resistance for the former, which is likely ascribable to its enhanced molecular ordering.

The J_{sc} values of the two cells are consistent with the external quantum efficiencies (EQEs) shown in Fig. 6SI. The two polymer have similar spectral profiles, with a photocurrent response ranging from 300 to 700 nm and three feature peaks at 350, 450 and 540 nm, thus suggesting that the harvested photons over the whole absorption spectrum can effectively contribute to the photocurrent of the final device. Moreover, an enhanced EQE is observed for PT12OH sample (EQE_{max} 81% vs

74%), suggesting an improved charge collection efficiency for the hydroxylated polymer, in line with the higher value of J_{sc} measured for the BHJ solar cells prepared with this polymer.

3.6. Photostability

Bulk heterojunction (BHJ) cell photoactive layers, consisting of electron- donor and electron-acceptor molecules mixed in a nanometer scale, usually suffer from long-term stability problems determined by morphological changes. These changes are particularly frequent when the polymeric cells are exposed to external thermal or illumination conditions [47] that produce adverse conformational changes in polymeric chains and a gradual loss of photoconversion efficiency. Thus the strategy adopted in this work to overcome the instability issues is that of using a self-assemblingpolymer, i.e. PT12OH, which is able to "freeze" the nanosized-morphology of the photoactive blend through inter- and intrachain hydrogen bonds. This strategy has some advantages, in particular a remarkable simplification of device fabrication, since the post-annealing thermal crosslinking [48], photocrosslinking [49] or chemical crosslinking [50] steps, reported in previous works, can be completely avoided. Indeed, the –OH functionality is able to reduce the side-chain flexibility and increases the thermal stability of the cells by decreasing the rotational freedom of the polymeric backbone.

The over-time thermal stability of polymer-based devices is shown in Fig. 9, where the power conversion efficiency (PCE) of both PT12Br and PT12OH are shown at different times. The initial performances obtained with the two polymers are comparable, but a striking difference can be observed upon exposure to heat: while PT12Br undergoes a sharp decrease in performance with heating over time, PT12OH retains an acceptable photoconversion efficiency even after 120 h at 120°C (66% of the initial value retained). This behaviour may be ascribed to the presence of hydrogen bond interactions between PT12OH side chains, which increase the phase transition temperatures (Table 4), allowing for the optimal morphology of the blend - obtained by the initial

annealing procedure - to be maintained throughout the entire accelerated aging process, thus resulting in a remarkable long-term stability of the final devices.

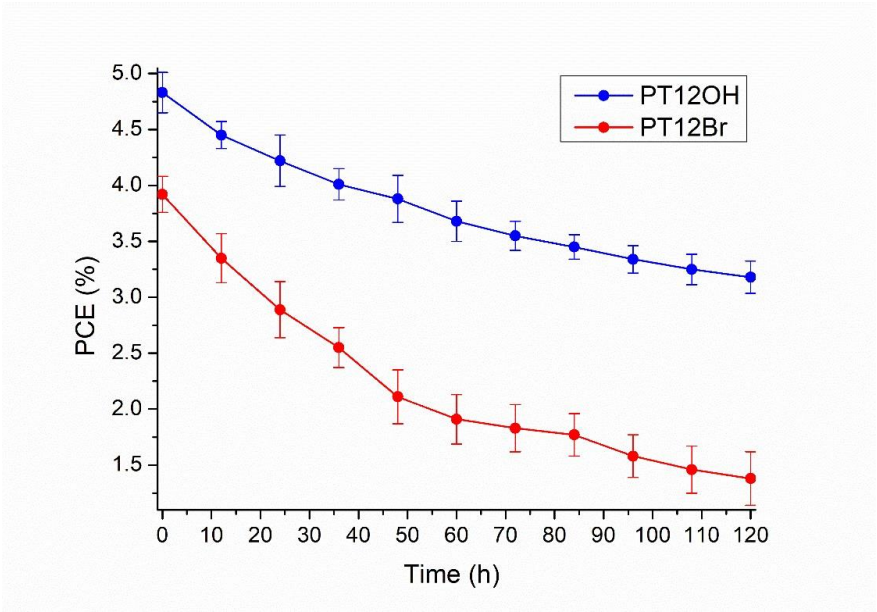

Fig. 9. Efficiencies of BHJ solar cells heated at 120°C (under vacuum) vs time. Ten devices of each type were prepared and tested.

SEM analysis, performed on photoactive blends (polythiophene:PCBM 1:1.25 (w/w)) evidences a similar behaviour of the two examined polymers before the accelerated aging procedure. Indeed, PT12Br (Fig. 10a) and PT12OH (Fig. 10c) blends show very similar morphologies, with a fine, uniform texture, ascribable to the formation of well-mixed homogeneous films. Conversely, thermally-aged samples show evident differences, with PT12Br (Fig. 10b) undergoing a noticeable change in structure, with the formation of nanometric aggregates (diameter ranging from 21.3 to 4.2 nm), while the PT12OH microstructure (Fig. 10d) remains substantially unchanged. EDX analysis shows no differences in the distibution of key elements (C, S, Br and O) at the micrometric level, confirming that aggregation takes place at the nanometric level for both samples.

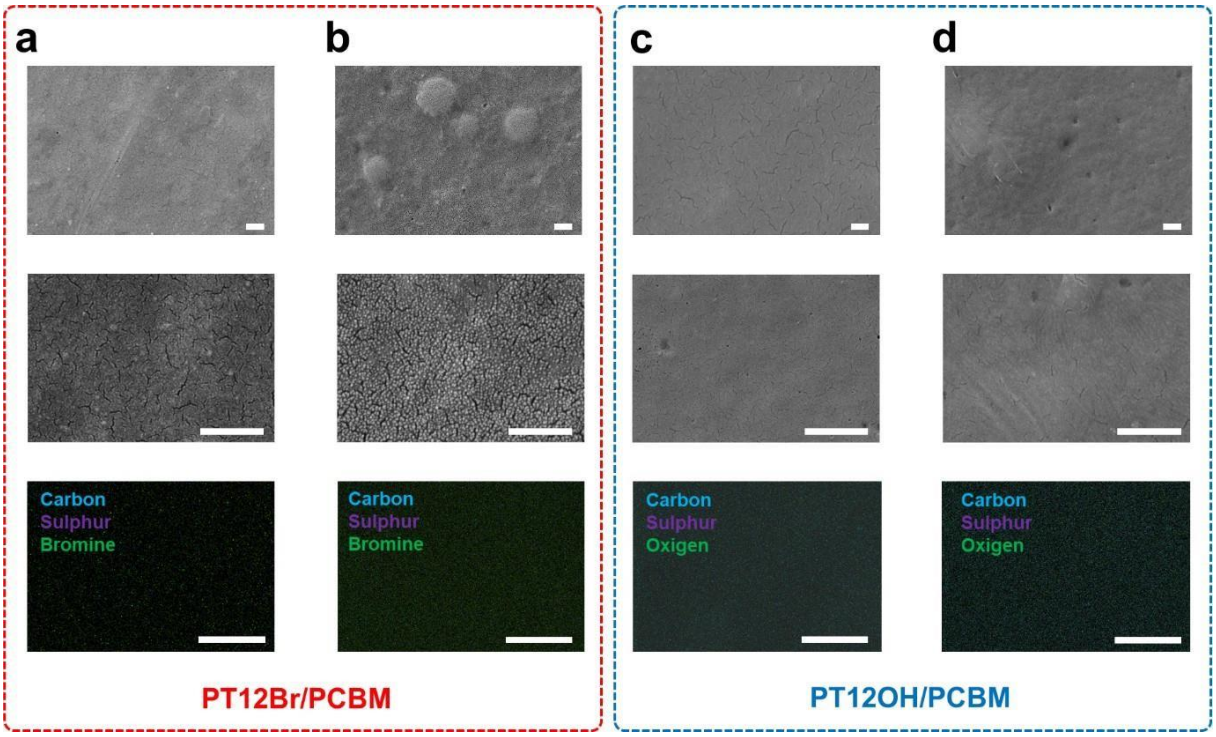

Fig. 10. The active layer surface structure of organic photovoltaic cells. FE-SEM at two different magnifications and EDX elemental mapping: (a) PT12Br/PCBM, (b) PT12Br/PCBM heated, (c) PT12OH/PCBM and (d) PT12OH/PCBM heated. (All scale bars are equal to 400 nm).

AFM analyses are in line with SEM results. The comparison between the topographical and phase images of PT12Br pristine (Fig. 11a) and heated (Fig. 11b) samples reveal the formation ofaggregates in the active layer after the aging procedure. Indeed, a marked increase in RMS roughness was observed on passing from the unheated (3.9±0.4 nm) to the heated sample (16.8±3.5nm). This increase was notably lower passing from the pristine PT12OH blend (Fig. 10c, RMS 3.5±0.3 nm) to the heated one (Fig. 10d, RMS 5.3±0.6 nm), probably because the morphologystabilization induced by –OH interactions makes it possible to preserve the well-developed ED/EA network, limiting a large aggregation of PCBM in the film. We can conclude that microstructural characterizations indicate negligible morphological changes in the nanoscale range for the hydroxylated sample, due to the stabilizing interactions between side chains.

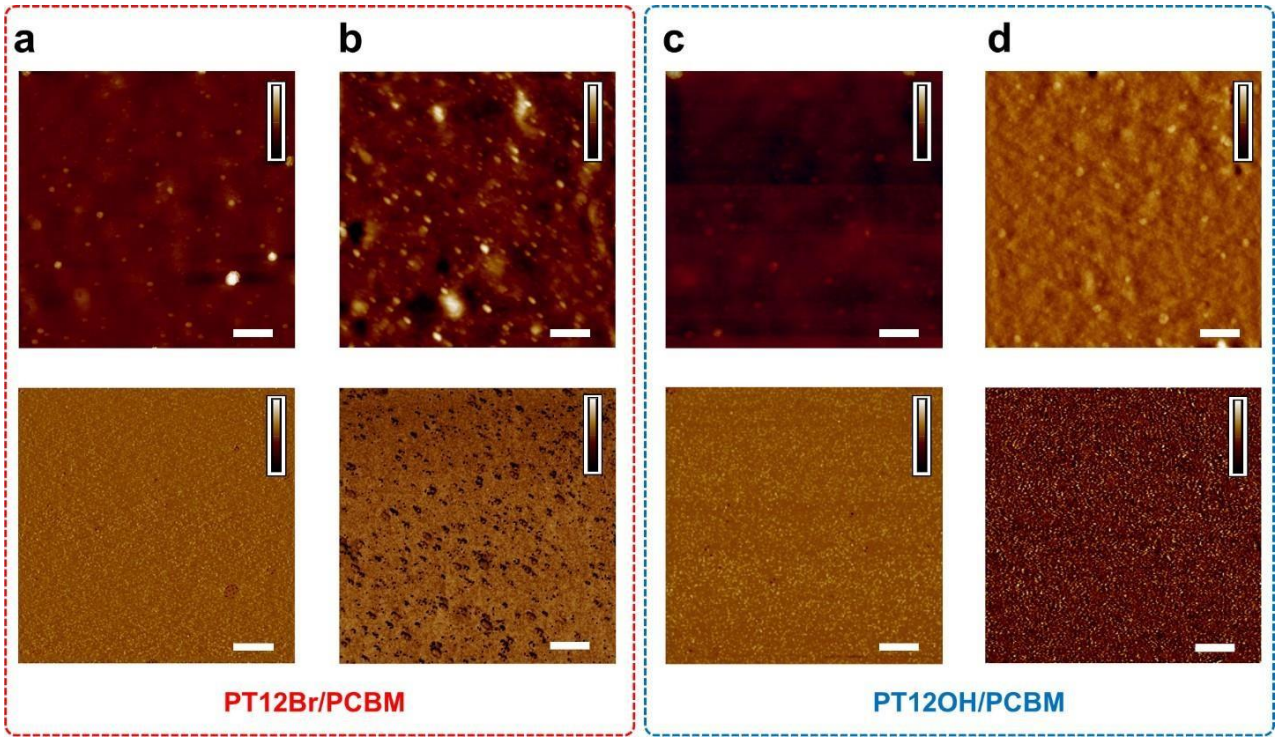

Fig. 11 AFM topographical and phase images of the active material layers obtained from: (a) PT12Br/PCBM, (b) PT12Br/PCBM heated, (c) PT12OH/PCBM and (d) PT12OH/PCBM heated. All scale bars are equal to 400 nm. The z-scales are equal to: (a) 11 nm and 20 degree, (b) 55 nmand 60 degree, (c) 8 nm and 10 degree and (d) 25 nm and 30 degree.

4. Conclusions

We synthesized two regioregular polythiophene derivatives functionalized with a -Br or –OH group at the end of a dodecamethylenic side chain. These polymers were completely characterized from the chemical, structural, morphological, and photoelectrical standpoints and were used as electron- donor materials in combination with $PC_{61}BM$ for the preparation of bulk heterojunction solar cells, which showed good photovoltaic performances and a broad photoresponse range. After a prolongedthermal treatment, the formation of PCBM aggregation and partial blend demixing, observed with the brominated polymer, was effectively suppressed using the corresponding hydroxy-

functionalized polythiophene, which led to a more stable device performance without resorting to any post-annealing thermal, chemical, or photocrosslinking procedure, while maintaining the good solubility of the polymer. The results of this study may be especially useful for the design and large-scale production of high-efficiency BHJ solar cells with long-term stability.

Acknowledgments

This study was partially supported by the First TEAM grant number POIR.04.04.00-00-5ED7/18- 00, conducted within the framework of the First TEAM programme of the Foundation for Polish Science (FNP), and co-financed by the European Union under the European Regional development Fund. The authors are also grateful for the support offered by the Canaletto programme (grant number PPN/BIL/2018/2/00035/U/00001), funded by the National Agency for Academic Exchange (NAWA) and the Italian Ministry of Foreign Affairs and International Cooperation (Farnesina), Project PO19MO13.

Declaration

The raw/processed data required to reproduce these findings cannot be shared at this time as the data also forms part of an ongoing study.

References

[1] R. Jaiswal, U. Saha, T. H. Goswami, A. Srivastava, N. Eswara Prasad, A unique extension of Suzuki-Sonogashira cross coupling reaction in developing acetylene terminated fullerene core star-like phenylene-alt-thiophene dyad materials and its photovoltaic properties, Polymer, 164 (2019) 39-58, https://doi.org/10.1016/j.polymer.2019.01.011.

[2] S. Yamamoto, H. Yasuda, H. Ohkita, H. Benten, S. Ito, S. Miyanishi, K. Tajima, K. Hashimoto, Charge generation and recombination in fullerene-attached poly(3-hexylthiophene)-based diblock copolymer films, J. Phys. Chem. C., 118 (2014) 10584-10589, https://doi.org/10.1021/jp4126683.

[3] W. L. Ma, C. Y. Yang, X. Gong, K. Lee, A. J. Heeger, Thermally stable, efficient polymer solar cells with nanoscale control of the interpenetrating network morphology, Adv. Funct. Mater., 15 (2005) 1617-1622, https://doi.org/10.1002/adfm.200500211.

[4] Z. Zhu, S. Hadjikyriacon, D. Waller, R. Gaudiana, Stabilization of film morphology in polymer-fullerene heterojunction solar cells, J. Macromol. Sci., A41 (2004) 1467-1487, https://doi.org/10.1081/MA-200035416.

[5] M. Drees, H. Hoppe, C. Winder, H. Neugebauer, N. S. Sariciftci, W. Schwinger, F. Schaffler, C. Topf, M. C. Scharber, Z. G. Zhu, R. Gaudiana, Stabilization of the nanomorphology of polymer–fullerene "bulk heterojunction" blends using a novel polymerizable fullerene derivative, J. Mater. Chem., 15 (2005) 5158-5163, https://doi.org/10.1039/B505361G.

[6] G. Griffini, J. D. Douglas, C. Piliego, T. W. Holcombe, S. Turri, J. M. J. Fréchet, J. L. Mynar, Long-term thermal stability of high-efficiency polymer solar cells based on photocrosslinkable donor-acceptor conjugated polymers, Adv. Mat., 23 (2011) 1660-1664, https://doi.org/10.1002/adma.201004743.

[7] W. Lai, C. Li, J. Zhang, F. Yang, F. J. M. Colberts, B. Guo, Q. M. Wang, M. Li, A. Zhang, R. A. J. Janssen, M. Zhang, W. Li, Diketopyrrolopyrrole-based conjugated polymers with perylene bisimide side chains for single-component organic solar cells, Chem. Mater., 29 (2017) 7073-7077, https://doi.org/10.1021/acs.chemmater.7b02534.

[8] G. Feng, J. Li, F. J. M. Colberts, M. Li, J. Zhang, F. Yang, Y. Jin, F. Zhang, R. A. J. Janssen, C. Li, W. Li, "Double-cable" conjugated polymers with linear backbone toward high quantum efficiencies in single-component polymer solar cells, J. Am. Chem. Soc., 139 (2017) 18647-18656, https://doi.org/10.1021/jacs.7b10499.

[9] W. Xu, L. Li, H. Tang, H. Li, X. Zhao, X. Yang, Solvent-induced crystallization of poly(3-dodecylthiophene): morphology and kinetics, J. Phys. Chem. B, 115 (2011) 6412-6420, https://doi.org/10.1021/jp201044b.

[10] J. H. Liu, M. Arif, J. H. Zou, S. I. Khondaker, L. Zhai, Controlling poly(3-hexylthiophene) crystal dimension: nanowhiskers and nanoribbons, Macromolecules, 42 (2009) 9390-9393, https://doi.org/10.1021/ma901955c.

[11] S. L. Liu, T. S. Chung, Crystallization and melting behavior of regioregular poly(3-dodecylthiophene), Polymer, 41 (2000) 2781-2793, https://doi.org/10.1016/S0032-3861(99)00490-5.

[12] S. Yue, G. C. Berry, R. D. McCullough, Intermolecular association and supramolecular organization in dilute solution. 1. regioregular poly(3-dodecylthiophene), Macromolecules, 29 (1996) 933-939, https://doi.org/10.1021/ma951008+.

[13] V. Causin, C. Marega, A. Marigo, L. Valentini, J. M. Kenny, Crystallization and melting behavior of poly(3-butylthiophene), poly(3-octylthiophene), and poly(3-dodecylthiophene), Macromolecules, 38 (2005) 409-415, https://doi.org/10.1021/ma048159+.

[14] Y. Guo, L. Wang, Y. Han, Y. Geng, Z. Su, Influence of molecular weight on polymorphs and temperature-induced structure evolution of regioregular poly(3-dodecylthiophene), Polym. Chem. 5 (2014) 1938-1944, https://doi.org/10.1039/C3PY01282D.

[15] H. Chen, C. Su, G. Shi, G. Liu, D. Wang, Nature of the double melting peaks of regioregular poly(3-dodecylthiophene), Eur. Polym. J., 99 (2018) 284-288, https://doi.org/10.1016/j.eurpolymj.2017.12.031.

[16] C. Yang, F. P. Orfino, S. A. Holdcroft, A phenomenological model for predicting thermochromism of regioregular and nonregioregular poly(3-alkylthiophenes), Macromolecules, 29 (1996) 6510-6517, https://doi.org/10.1021/ma9604799.

[17] K. C. Park, K. Levon, Order−disorder transition in the electroactive polymer poly(3-dodecylthiophene), Macromolecules, 30 (1997) 3175-3183, https://doi.org/10.1021/ma961322j.

[18] K. C. Park, K. Levon, Liquid crystallinity in the electro-active polymer, poly(3-dodecylthiophene), Mol. Cryst. Liq. Cryst. 319 (1998) 61-73, https://doi.org/10.1080/10587259808045648.

[19] P. Bauerle, F. Wurtner, S. Heid, Facile synthesis of 3-(ω-haloalkyl)thiophenes as key building blocks for functionalized thiophenes and polythiophenes, Angew. Chem., Int. Ed. Engl. 29 (1990) 419-420, https://doi.org/10.1002/anie.199004191.

[20] F. Pierini, M. Lanzi, P. Nakielski, S. Pawlowska, O. Urbanek, K. Zembrzycki, T. A. Kowalewski, Single-material organic solar cells based on electrospun fullerene-grafted polythiophene nanofibers, Macromolecules, 50 (2017) 4972-4981, https://doi.org/10.1021/acs.macromol.7b00857.

[21] R. D. McCullough, R. D. Lowe, M. Jayaraman, D. L. Anderson, Design, synthesis, and control of conducting polymer architectures: structurally homogeneous poly(3-alkylthiophenes), J. Org. Chem., 58 (1993) 904-912, https://doi.org/10.1021/jo00056a024.

[22] R. S. Lowe, S. M. Khersonsky, R. D. McCullough, A simple method to prepare head-to-tail coupled, regioregular poly(3-alkylthiophenes) using grignard metathesis, Adv. Mater., 11 (1999) 250-253, https://doi.org/10.1002/(SICI)1521-4095(199903)11:3<250::AID-ADMA250>3.0.CO;2-J.

[23] F. Bertinelli, P. Costa-Bizzarri, C. Della-Casa, M. Lanzi, Analysis of UV–Vis spectral profiles of solvatochromic poly[3-(10-hydroxydecyl)-2,5-thienylene], Spectrochim. Acta Part A, 58 (2002) 583-592, https://doi.org/10.1016/S1386-1425(01)00560-1.

[24] M. Lanzi, P. Costa-Bizzarri, C. Della-Casa, L. Paganin, A. Fraleoni, Synthesis, characterization and optical properties of a regioregular and soluble poly[3-(10-hydroxydecyl)-2,5- thienylene], Polymer, 44 (2003) 535-545, https://doi.org/10.1016/S0032-3861(02)00800-5.

[25] H. Tachibana, N. Hosaka, Y. Tokura, Hysteretic thermochromism of regioregular poly(3-alkylthiophene) thin films, Macromolecules, 34 (2001) 1823-1827, https://doi.org/10.1021/ma0009449.

[26] Y. Furukawa, M. Akimodo, I. Harada, Vibrational key bands and electrical conductivity of polythiophene, Synth. Met., 18 (1987) 151-156, https://doi.org/10.1016/0379-6779(87)90870-8.

[27] T. A. Chen, X. Wu, R. D. Rieke, Regiocontrolled synthesis of poly(3-alkylthiophenes) mediated by rieke zinc: their characterization and solid-state properties, J. Am. Chem. Soc., 117 (1995) 233-244, https://doi.org/10.1021/ja00106a027.

[28] L. Jaquinod, O. Siri, R. G. Khoury, K. M. Smith, Linear fused oligoporphyrins: potential molecular wires with enhanced electronic communication between bridged metal ions, Chem. Commun., (1998) 1261-1262, https://doi.org/10.1039/A801676C.

[29] B. J. Schwartz, Conjugated polymers as molecular materials: how chain conformation and film morphology influence energy transfer and interchain interactions, Ann. Rev. Phys. Chem. 54 (2003), 141-172, https://doi.org/10.1146/annurev.physchem.54.011002.103811.

[30] R. Qian, Aspects of molecular design of conducting polymers, Makromol. Chem., Macromol. Symp., 33 (1990) 327-339, https://doi.org/10.1002/masy.19900330128.

[31] J. Clark, C. Silva, R. H. Friend, F. C. Spano, Role of intermolecular coupling in the photophysics of disordered organic semiconductors: aggregate emission in regioregular polythiophene, Phys. Rev. Lett., 98 (2007), 206406, https://doi.org/10.1103/PhysRevLett.98.206406.

[32] J. Clark, J. F. Chang, F. C. Spano, R. H. Friend, C. Silva, Determining exciton bandwidth and film microstructure in polythiophene films using linear absorption spectroscopy, Appl. Phys. Lett. 94 (2009) 163306, https://doi.org/10.1063/1.3110904.

[33] F. C. Spano, Absorption in regio-regular poly(3-hexyl)thiophene thin films: Fermi resonances, interband coupling and disorder, Chem. Phys., 325 (2006) 22-35, https://doi.org/10.1016/j.chemphys.2005.08.019.

[34] B. Xu, S. Holdcroft, Molecular control of luminescence from poly(3-hexylthiophenes), Macromolecules, 26 (1993) 4457-4460, https://doi.org/10.1021/ma00069a009.

[35] J. Pommerehne, H. Westweber, W. Guss, R. F. Mahrt, H. Bassler, M. Porsch, J. Daub,Efficient two layer leds on a polymer blend basis, Adv. Mater., 7 (1995) 551-554, https://doi.org/10.1002/adma.19950070608.

[36] T. V. Richter, C. H. Braun, S. Link, M. Scheuble, E. J. W. Crossland, F. Stelzl, U. Wuerfel, S. Ludwigs, Regioregular polythiophenes with alkylthiophene side chains, Macromolecules, 45 (2012) 5782-5788, https://doi.org/10.1021/ma2026644.

[37] M. C. Scharber, D. Muehlbacher, M. Koppe, P. Denk, C. Waldauf, A. J. Heeger, C. J. Brabec, Design rules for donors in bulk-heterojunction solar cells-towards 10% energy-conversion efficiency, Adv. Mater., 18 (2006) 789-794, https://doi.org/10.1002/adma.200501717.

[38] P. Schilinsky, C. Waldauf, J. Hauch, C. J. Brabec, Simulation of light intensity dependent current characteristics of polymer solar cells, J. Appl. Phys., 95 (2004) 2816-2819, https://doi.org/10.1063/1.1646435.

[39] J. L. Bredas, Mind the gap!, Mater. Horiz., 1 (2014) 17-19, https://doi.org/10.1039/C3MH00098B.

[40] R. Holze, Optical and electrochemical band gaps in mono-, oligo-, and polymeric systems: a critical reassessment1, Organometallics, 33 (2014) 5033-5042, https://doi.org/10.1021/om500604z.

[41] R. J. Kline, D. M. DeLongchamp, D. A. Fischer, E. K. Lin, L. J. Richter, M. L. Chabinyc, M. F. Toney, M. Heeney, I. McCulloch, Critical role of side-chain attachment density on the order and device performance of polythiophenes, Macromolecules, 40 (2007) 7960-7965, https://doi.org/10.1021/ma0709001.

[42] B. D. Cullity, in Elements of X-Ray Diffraction, Addison-Wesley, Reading, MA 1978, ISBN/ISSN: 9780131788183.

[43] S. Nam, S. Park, H. Kim, J. H. Lee, Y. Lim, Strong addition effect of charge-bridging polymer in polymer:fullerene solar cells with low fullerene content, RSC Adv., 4 (2014) 24914-24921, https://doi.org/10.1039/C4RA01918K.

[44] H. J. Snaith, A. C. Arias, A. C. Morteani, C. Silva, R. H. Friend, Charge generation kineticsand transport mechanisms in blended polyfluorene photovoltaic devices, Nano Lett., 2 (2002) 1353-1357, https://doi.org/10.1021/nl0257418.

[45] N. D. Treat, C. G. Shuttle, M. F. Toney, C. G. Hawker, M. L. Chabinyc, In situ measurement of power conversion efficiency and molecular ordering during thermal annealing in P3HT:PCBM bulk heterojunction solar cells, J. Mater. Chem., 21 (2011) 15224-15231, https://doi.org/ 10.1039/C1JM12677F.

[46] H. Zhou, L. Yang, W. You, Rational design of high performance conjugated polymers for organic solar cells, Macromolecules, 45 (2012) 607-632, https://doi.org/10.1021/ma201648t.

[47] I. Fraga Dominguez, A. Distler, L. Luer, Stability of organic solar cells: the influence of nanostructured carbon materials, Adv. Energy Mater., 7 (2017) 1601320, https://doi.org/10.1002/aenm.201601320.

[48] B. J. Kim, Y. Miyamoto, B. W. Ma, J. M. J. Fréchet, Photocrosslinkable polythiophenes for efficient, thermally stable, organic photovoltaics, Adv. Funct. Mater., 19 (2009) 2273-2281, https://doi.org/10.1002/adfm.200900043.

[49] C. Piliego, T. W. Holcombe, J. D. Douglas, C. H. Woo, P. M. Beaujuge, J. M. J. Fréchet, Synthetic control of structural order in n-alkylthieno[3,4-c]pyrrole-4,6-dione-based polymers for efficient solar cells, J. Am. Chem. Soc., 132 (2010) 7595-7597, https://doi.org/10.1021/ja103275u.

[50] S. Miyanishi, K. Tajima, K. Hashimoto, Morphological stabilization of polymer photovoltaic cells by using cross-linkable poly(3-(5-hexenyl)thiophene), Macromolecules, 42 (2009) 1610-1618, https://doi.org/10.1021/ma802839a.

Declaration of interests

☒ The authors declare that they have no known competing financial interests or personal relationships that could have appeared to influence the work reported in this paper.

☐ The authors declare the following financial interests/personal relationships which may be considered as potential competing interests:

[Supporting Information]

Efficient and thermally stable BHJ solar cells based on a soluble hydroxy-functionalized regioregular polydodecylthiophene

Massimiliano Lanzi[*,†] *and Filippo Pierini*[§]

[†]Department of Industrial Chemistry "Toso Montanari", Alma Mater Studiorum-University of Bologna, 40136 Bologna, Italy

[§]Department of Biosystems and Soft Matter, Institute of Fundamental Technological Research, Polish Academy of Sciences, Warsaw 02-106, Poland

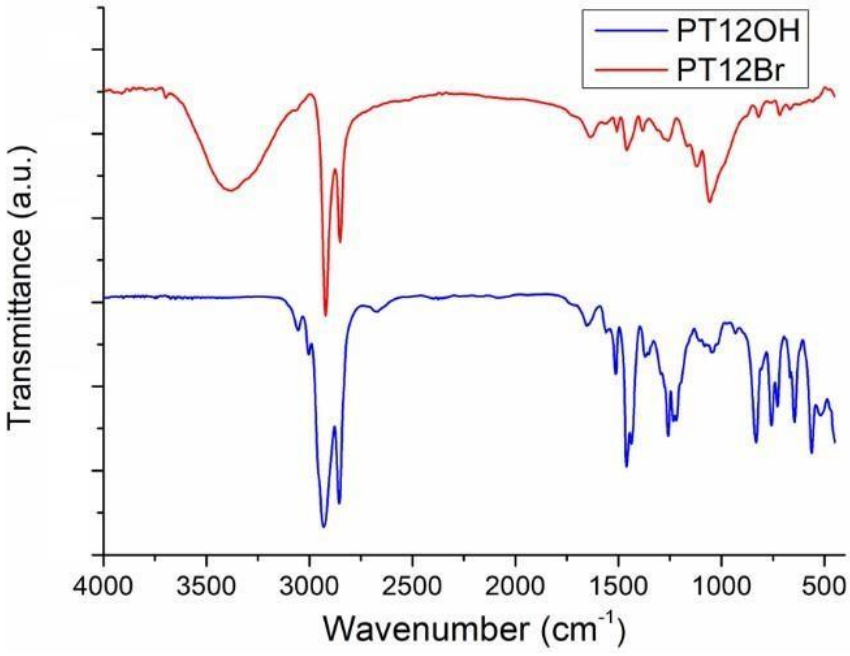

Figure 1SI. FT-IR spectra of the synthesized polymers.

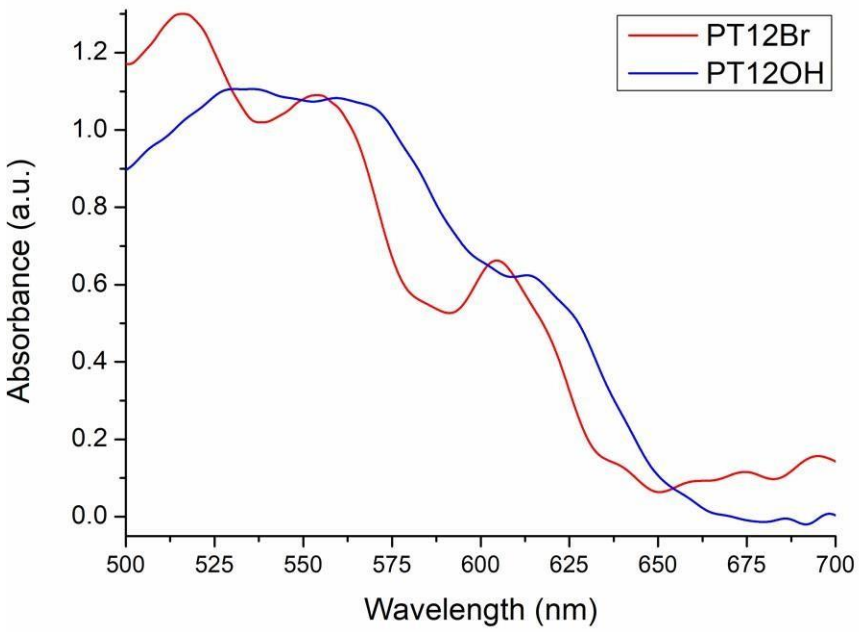

Figure 2SI. Deconvolution of UV-Vis spectra of PT12Br and PT12OH in film (low energies range).

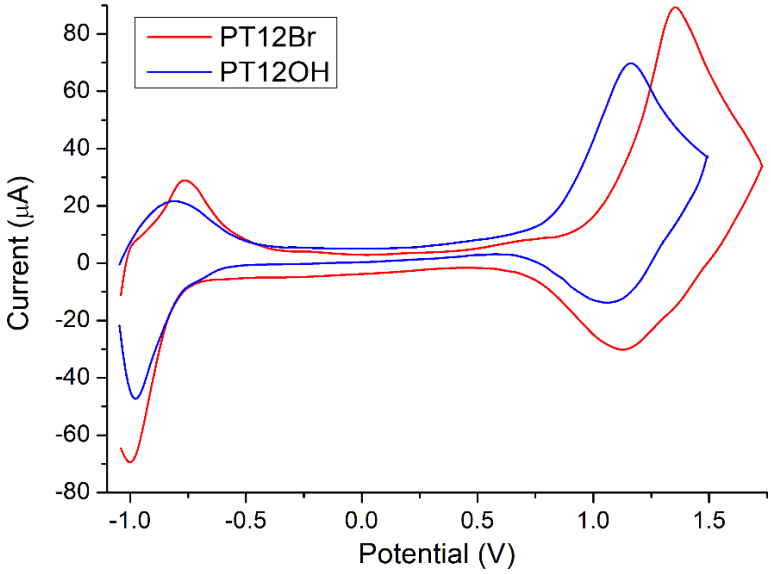

Figure 3SI. Cyclic voltammograms of PT12Br and PT12OH polymers.

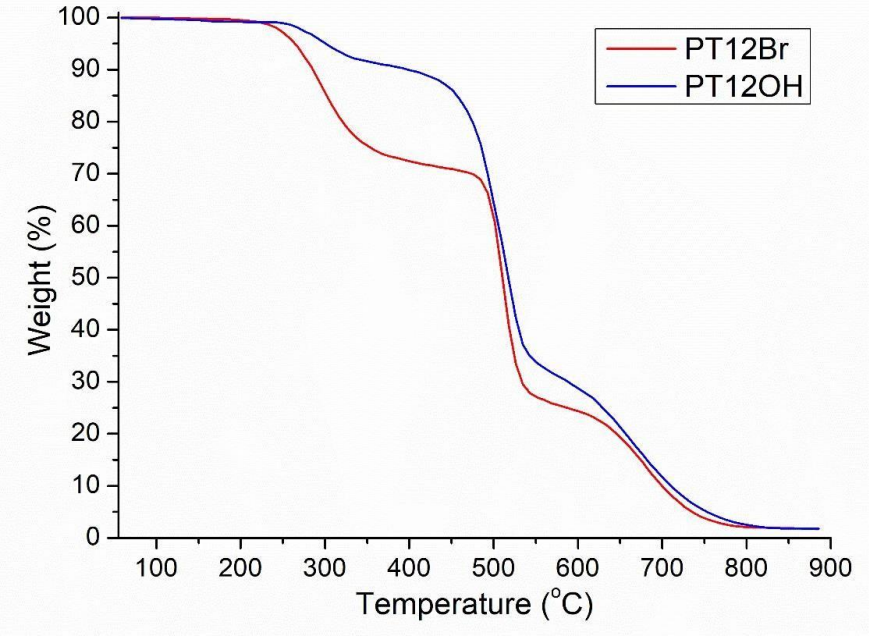

Figure 4SI. TGA thermograms of polymers under air.

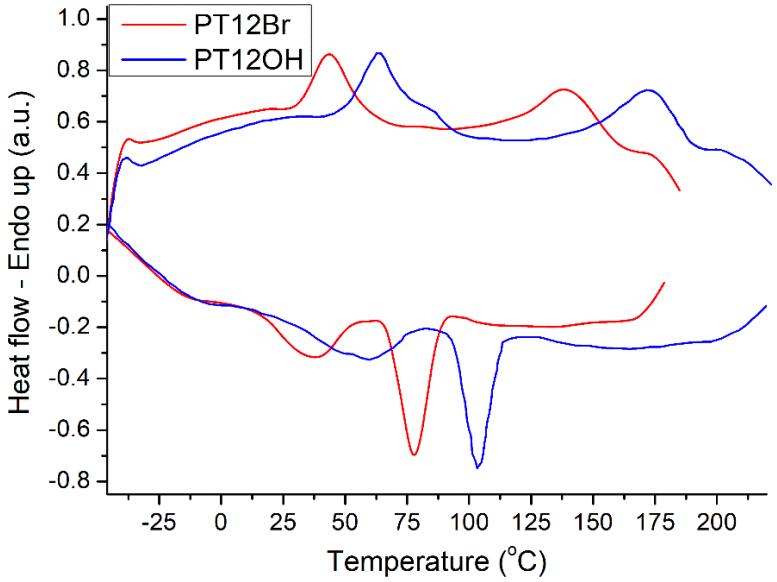

Figure 5SI. DSC thermograms of polymers under nitrogen (second scan).

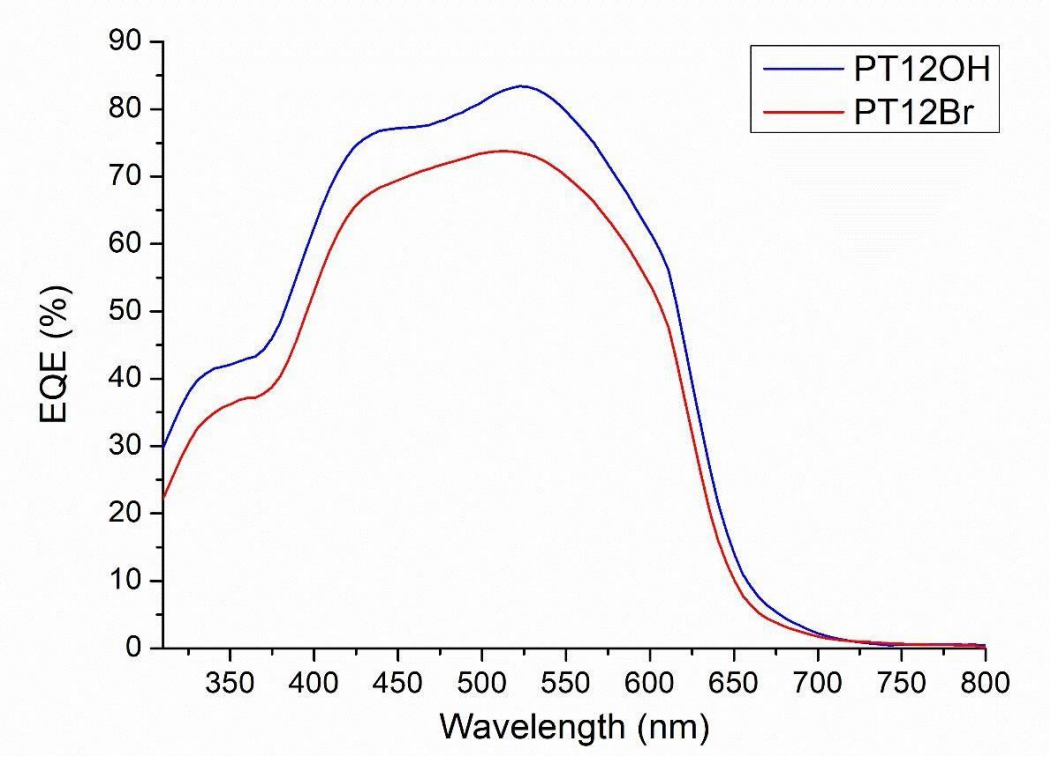

Figure 6SI. External quantum efficiency (EQE) spectra of polymer/PCBM devices.